01 Jan 1980

Abutment-thermal interaction of a composite bridge

David B. Lewis

ABUTMENT-THERMAL INTERACTION OF A COMPOSITE BRIDGE

BY

DAVID B. LEWIS, 1956-

A THESIS

Presented to the Faculty of the Graduate School of the

UNIVERSITY OF MISSOURI-ROLLA

In Partial Fulfillment of the Requirements for the Degree

MASTER OF SCIENCE IN CIVIL ENGINEERING

1980

Approved by

Jack H. Emanuel (Advisor)

John L. Best

Myron G. Perry

PUBLICATION THESIS OPTION

This thesis has been prepared in the style utilized by the Journal of the Structural Division, American Society of Civil Engineers. Pages iii, iv, and 1 through 36 will be presented for publication in that journal. Appendices A, B, and C have been added for purposes normal to thesis unity.

CIVIL ENGINEERING ABSTRACT

A two-span test structure, with tie-rods to similate approach-slab forces, was subjected to thermal loading. The resultant strains and deflections are correlated with those obtained from a prior theoretical study. It was concluded that the theoretical procedure provides a rational method for predicting the thermal behavior of composite-girder bridge structures.

ABUTMENT-THERMAL INTERACTION OF A COMPOSITE BRIDGE

By Jack H. Emanuel and David B. Lewis

ABSTRACT

This experimental investigation was conducted to substantiate a prior study of environmental stresses induced in composite-girder bridge structures. The objectives of the study were to subject a two-span test structure, with tie-rods to simulate approach-slab forces, to thermal loading, and to correlate the resultant strains and deflections with those obtained from the theoretical study. Three theoretical cases were considered for strain calculations: (a) both the slab and the beam in plane stress, (b) the slab in plane strain and the beam in plane stress, and (c) the slab in some state between plane stress and plane strain (partially restrained) and the beam in plane stress.

The experimental results and theoretical values were in reasonable agreement. Closest agreement for the slab and for the beam was given by case b and case c, respectively. It was concluded that the theoretical procedure provides a rational method for predicting the thermal behavior of composite-girder bridge structures and can be applied with reasonable confidence when used with realistic temperature profiles, material properties, and substructure stiffness characteristics.

KEYWORDS: Bridges (approach-slab); Bridges (composite); Bridge decks; Bridge movements; Bridges (structural); Composite beams; Concrete (reinforced); Temperature distribution; Thermal coefficient of expansion; Thermal strains; Thermal stresses.

ACKNOWLEDGEMENTS

The author wishes to express his appreciation to Dr. Jack H. Emanuel, Chairman of the Graduate Committee, for his encouragement, advice, and patient editing of this manuscript. Thanks are also due to Drs. John L. Best and Myron G. Parry for serving on the Graduate Committee.

Very special thanks are due to Drs. Peter G. Hansen and J. Leroy Hulsey, without whose help and encouragement this study could never have materialized, and to Mr. Ken Haas for his many hours of work on the design and fabrication of data recording equipment.

TABLE OF CONTENTS

Page

APPENDICES

LIST OF ILLUSTRATIONS

LIST OF TABLES

APPENDICES

ABUTMENT-THERMAL INTERACTION OF A COMPOSITE BRIDGE

By Jack H. Emanuel,[1] F. ASCE, and David B. Lewis,[2]

INTRODUCTION

A major factor in the movement of bridges is temperature change. This temperature change induces thermal stresses unless the structure is homogeneous, free of restraints, and of constant temperature; nonexistent conditions for a composite design structure. Thus, designers try to anticipate structural behavior, and attempt to provide for structural movements by using a variety of supporting and expansion devices (5).

Field observations show that these attempts are very often unsuccessful (27, 28, 30). Abutment movements caused by compaction, settling, or shifting of approach fill; growth or expansion of approach slabs; and "frozen" supporting and expansion devices are common observations. The significance of the combined effect of the resultant stresses and thermally induced stresses is often manifested in a variety of types of bridge distress. Some investigators have reported that thermally induced stresses in a composite design structure can reach 30 to 40 percent of the design strength (3, 16, 30).

One design which has become popular in recent years eliminates expansion devices by connecting the superstructure to a flexible substructure with either pinned or integral connections at the abutments.

---

[1]Prof. of Civil Engrg., Univ. of Missouri-Rolla, Rolla, Mo.

[2]Graduate Teaching Asst., Univ. of Missouri-Rolla, Rolla, Mo.

Thus, the entire bridge moves as a single unit. As with structures with expansion type supporting devices, if the approach slabs bind the abutments, a large external force on the ends of the structure may result when the approach slab and the structure both expand as a result of increasing temperatures.

Thermally induced stresses have been the subject of a number of investigations in the past several years (2, 3, 4, 11, 12, 13, 14, 15, 16, 18, 19, 22, 23, 24, 25, 26, 28, 29, 30, 31). Those conducted in Australia, New Zealand, Europe, and Canada have principally been concerned with concrete box-grider bridges rather than with concrete-steel composite bridges. Although the heat transfer analysis is similar for the two types of construction, the determination of strains and stresses is much more complex for a composite design structure.

Because of the increased usage of bridge structures supported by flexible substructures and the concern of design engineers regarding bridge behavior and induced stresses associated with bridges of this type, a study was conducted at the University of Missouri-Rolla to explore the feasibility of developing rational design criteria for bridges with Semi-Integral end bents. It was concluded that development of rational design criteria for bridges with Semi-Integral end bents is feasible, but the anticipated cost precluded continuation of subsequent phases to fruition as desired (6). However, subsequent rigorous studies (7, 8, 16, 17) investigated thermally induced stresses from a theoretical standpoint. A later investigation correlated experimental results obtained from a model test structure subjected to thermal loading with calculated values obtained from the theoretical approach, and provided substantiative data toward acceptance of the theoretical procedure in

development of rational design criteria (9, 30).

This study and a current on-going study were initiated to extend the areas of experimental-theoretical correlation, utilizing the test structure of the prior investigation. The objective of this study was to develop correlative experimental-theoretical data on the combined effect of approach slab thrust and thermal loading by a) restraining the abutments of the two-span laboratory test structure with tie rods, simulating approach slab thrust, b) subjecting the structure to thermal loading, and c) correlating the experimental results with calculated values obtained by utilizing the theoretical study.

TEST STRUCTURE

The test structure utilized was a 45-in. (114-cm) wide by 15 ft - 15 ft (4.6 m - 4.6 m) two-span continuous composite-design bridge constructed for a prior investigation conducted in the Civil Engineering Structural Laboratory of the Engineering Research Laboratory, University of Missouri-Rolla (9, 30). A curved steel plate and pintle bearing was used at the pier, and integral abutments were used at the ends. The structure was designed and constructed as an adequate rather than true model.

The abutment assembly consisted of a 6 x ½-in. (152 x 13-mm) steel-plate pile cap welded to three 5 x ½ x 72-in. (13 x 1.3 x 183-cm) steel-bar piling buried 66-in. (168-cm) in a 7 x 3 x 6-ft (2.1 x 0.9 x 1.8-m) sandbox of uniform density. As the steel-pile cap was bolted to the substructure stringers, the abutment assembly simulated an integral stub abutment with flexible piling.

The pier group was composed of three 2-in. (51-mm) diameter by

76½-in. (193-cm) long standard pipe sections spaced 20 in. (51 cm) on center and welded to a 12 x ½-in. (305 x 13-mm) base plate anchored to the floor. A 6 x ½-in. (152 x 13-mm) plate was used as a pier cap. The pier simulated a cantilever beam fixed to the existing floor. The cantilever simulation for the pier agrees with the fact that in the field most piers have a relative point of fixity and the portion above this point acts as a cantilever.

The superstructure was composed of three M6 x 4.4 steel stringers spaced 20 in. (51 cm) on center, with a 1.5-in. (38-mm) thick reinforced concrete deck. Ten sets of C4 x 5.4 channels were used for the diaphragms as shown in Fig. 1. Shear connectors consisted of 3/8-in. (10-mm) diameter by 7/8-in. (22-mm) studs spaced at 4 in. (10 cm) on center, except for high tensile zones.

The reinforced concrete deck was limited to a depth of 1.5 in. (38 mm) to prevent the deck from becoming too stiff in relation to the stringers. Two layers of 16-gauge 2-5/8-in. (68-mm) longitudinal by 2-in. (51-mm) transverse galvanized welded wire mesh were selected for the reinforcement. The top layer of mesh was positioned ¼-in. (6-mm) from the top of the finished deck, and the lower layer was set 1¼-in. (32-mm) from the top of the deck.

The concrete mix was composed of 20.6 lb (91.7 N) water, 34.6 lb (154 N) cement, 68.0 lb (303 N) sand, 68.0 lb (303 N) (3/8-in. [10-mm] nominal maximum size) crushed limestone, and 4 cc of air entraining agent. The concrete had a 28-day compressive strength of 4400 psi (30 360 kPa) and an air content of 5-1/2 $\pm$ 1-1/2 percent.

Four 1¼-in. (32-mm) diameter by 30-ft (9.1-m) long steel rods were used to simulate approach slab thrust on the abutments. These rods

were anchored by four 1½-in. (38.mm) diameter by 6-in. (15-cm) long tubes welded to the abutment caps at 15 in. (38 cm) centers. The dead load of the rods was supported by two wooden supports at the third points of the rods. To assure uniform seating and symmetrical loading from the rods, the rods were uniformly pretensioned to a specified force. The rods were threaded at the ends and thus pretensioned by sequential nut tightening immediately prior to each load sequence.

INSTRUMENTATION

Instrumentation was installed to record temperatures, strains, and displacements at selected points on the structure. To achieve this, thermistors, electrical resistance strain gages, and dial indicators were used. Data recording equipment consisted of four 10-channel Automation Industries Model SB-1 switch and balance units connected to an Automation Industries Model P-350 strain indicator, a 10-channel Baldwin-Lima-Hamilton Model 225 switch and balance unit connected to a Baldwin-Lima-Hamilton Model 120C strain indicator, an 8-channel Strain Sert switch, balance, and strain indicator, and a 100-channel thermistor stepping unit connected to a digital voltmeter (Dana Model 5400).

Two types of carbon-steel temperature-compensated SR-4 strain gages were used. The first type was Micro-Strain Model 6C-2x2-120 w/1 with a gage factor of 2.05, resistance of 120 ohms, grid size of 1/4 x 1/4-in. (6.4 x 6.4-mm) and an overall size of 3/8-in. by 5/16-in. (9.5 x 7.9-mm). The second type of strain gages was Baldwin-Lima-Hamilton Model FAE-25-12-56EWL with a gage factor of 2.06, resistance of 120 ohms, grid size of 1/8 x 9/32-in. (3.2 x 7.1-mm), and an overall size of 9/16 x

¼-in. (14.3 x 6.4-mm). The Micro-Strain gages were used on the bridge structure, while the BLH gages were used on the rods connecting the abutments.

The adhesive used for the Micro-Strain gages was Micro-Measurements M-Brand AE-15 two-part epoxy. This epoxy exhibits essentially creep-free performance up to 200° F (93° C) when cured at temperatures 25° F (14° C) greater than maximum operating temperatures. The adhesive used for the BLH gages was Micro-Measurements M-Brand AE-10 two-part epoxy, adequately cured at room temperature for this application.

Fenwal Uni-Curve No. UUA 33J1 thermistors were selected for the temperature sensors. These thermistors are epoxy encapsulated temperature sensitive resistors with a maximum spherical diameter of 0.095 in. (2.4 mm), resistance tollerance of ± 1 percent, and a temperature tolerance of ±0.4° F (0.22° C) over a range of 30-175° F (-1.1-79° C). Actual temperature values were obtained from observed values by a computer reduction utilizing logarithmic equations.

A two-part metal filled epoxy was used to attach the thermistors to their base locations in order to provide better heat conduction from the base material to the thermistor. A 100-channel stepping unit interfaced the thermistor leads to a digital voltmeter. Observed values were hand recorded.

Transducers embedded in the deck to measure strain and temperature were fabricated by mounting a strain gage and thermistor to a glass microscope slide. Beeswax was used to waterproof and protect the strain gage and a two-part steel-filled epoxy was used to attach the thermistor to the slide. The 1 x 3 x 1/10-in. (25 x 76 x 2.5-mm) glass slides, with a coefficient of linear thermal expansion of 5 x $10^{-6}/^{o}$ F (9 x $10^{-6}/^{o}$ C),

a thermal conductivity of 0.53 BTU/hr-ft-^{o}F (0.92 W/m-^{o}C), and a Young's Modulus of 10.3 x 10^{6} psi (71 x 10^{6} kPa), were selected because of the similarity of their thermal conductivity and coefficient of thermal expansion to that of the concrete. Slots were cut in the sides of the slides to provide a better mechanical bond to the deck concrete.

For confirmation of uniaxial stress and a uniform temperature gradient, four strain gages, equally spaced around the perimeter, and two thermistors, at the top and bottom surfaces, were mounted to each abutment tie-rod.

The total longitudinal deck deflection and the vertical deflection at the midspans were recorded by using dial indicators with a least count of 0.001 in. (0.025 mm). The indicators for vertical deflection were mounted on wooden standards, whereas the indicators at the abutments were attached to metal channels that were rigidly attached to the sandbox frame.

INSTRUMENTATION ORIENTATION

Five locations were chosen for the placement of the transducer groups as shown in Fig. 2. Two groups were distributed through the deck midway between the stringers, and the other three groups were placed on and immediately over the center stringer. Both thermistors and strain gages were used in each group. Slab transducers consisted of a glass microscope slide, strain gage, and thermistor as shown in Fig. 3.

Induced strains were read at the top, bottom, and four intermediate points of the slab and at the top and bottom of the stringer at locations 2, 3, and 4. At locations 1 and 5, midway between

center and outside stringers, slab transducers were placed in 4-in. (10-cm) wide by 9-in. (23-cm) long cantilever temperature-reference bars enclosed on the two sides and the end by ½-in. (13-mm) thick flexible styrofoam. Wire mesh was omitted in these bars so that the concrete could expand freely under unrestrained thermal expansion. The styrofoam produced essentially no resistance to small expansive movements and provided insulation between the boundaries.

Instrumentation locations 2, 3, and 4 were at sections along the center stringer. As noted above, strain gages and thermistors were placed at six points vertically through the deck slab. The sixth, or lowest point, was the interface between the slab and the stringer, and at this point two gages and one thermistor were attached to the top of the stringer flange. Seven thermistors were evenly spaced down the stringer web, and two were attached to the bottom flange; one at the outer edge of the flange and the other directly beneath the web. Strain gages mounted on the top and bottom flanges were spaced ¼-in. (6-mm) on each side of the centerline of the flange. A typical plan view and an elevation of this instrumentation are shown in Fig. 4. The slab transducers were staggered to avoid excessive congestion and placement problems.

Each abutment tie-rod was instrumented with four strain gages, equally placed around the perimeter of the rod, and two thermistors, placed at the top and bottom of the rod, to allow confirmation of uniaxial stress and a uniform temperature gradient. This entire instrumentation group was placed 14 ft (4.3 m) from the north abutment of the bridge.

Dial indicators with a least count of 0.001 in. (0.025 mm) were used to measure the vertical deflection of the center stringer at

midspans (locations 2 and 4) and the longitudinal deck displacements at each abutment. The total deck movement at the bearing elevation was obtained by summing the abutment displacements.

Two thermistors were also positioned at 2 and 12 in. (5 and 30 cm) above the top of the deck and two at 12 and 30 in. (30 and 76 cm) below the deck to give an indication of the still air temperature and thermal gradients around the bridge.

HEAT SOURCE

Radiation heating from 120 General Electric model 250R40 (250 watt) infared reflector heat lamps was used to thermally load the test structure. The lamps were placed in four rows along the length of the bridge and were spaced 12 in. (30 cm) center-to-center both longitudinally and transversely for uniformity of approximately 150^{o} F (65.6^{o} C). Alternate rows were staggered 6 in. (15 cm) to provide a more uniform radiation level. The bulb faces were placed 20 in. (51 cm) above the deck in accordance with the manufacturer's recommendation that the distance of the lamp from the heated subject be at least 1.6 times the lamp spacing for uniform radiation distribution. Radiation heating was choosen rather than a constant temperature source, because it was simpler and approximated actual field conditions imposed by the sun.

The lamps were divided into five circuits; each with a 240-volt Variac transformer to vary the thermal loading. The 115-volt lamps were connected in series by pairs to split the 240-volt transformer output. These pairs were then connected in parallel to complete a transformer string. The voltage drop through the wires was less than one percent because the transformer leads were connected to the center of a bulb

string. All leads and couplers consisted of 12-gauge wire.

To obtain uniform heat flux, the outside circuits required a higher voltage input than the interior circuits because the overlap of radiant energy along the edges was not as pronounced as in the center.

To check the uniformity of the heat flux, a heat receptor was fabricated of a 5 x 3 x 1-in. (127 x 76 x 25-mm) carbon steel bar painted flat black on the upper face. Thermistors were placed on both faces, and the bar was encased in styrofoam to prevent the loss of heat from the sides and to limit the convection to the top and bottom surfaces. The painted side was exposed to the radiation and the opposite face to ambient air. The uniformity of radiant energy was checked by observing the steady state temperatures of the receptors when placed at different points on the bridge deck. Voltages were then adjusted as necessary to give a uniform heat flux.

TESTING PROCEDURE

Before each testing cycle, the laboratory was sealed to eliminate any outside drafts--heating and air return ducts sealed, door cracks taped, and outside openings covered with plastic. Thus, the only source of forced convection would be air currents caused by either thermal gradients above and below the test structure developing into a cyclic draft as a result of the laboratory's high ceiling or by cross currents developing between the warm and cool ends of the large laboratory.

A test cycle then consisted of the following sequential steps.

1. All strain gages and dial indicators were "zeroed" and the bridge and ambient air thermistor readings recorded for use as the

reference temperatures at zero strain.

2. Each of the four rods was tensioned to a uniform tensile strain equal to the thermal elongation which would result solely from the temperature change of the rods during the test, and strain gage readings recorded for possible future reference. The force in the rods varied during the test--decreasing as the shaded rods elongated when their temperature increased, increasing as a result of the larger differential movement of the superstructure (subjected to a greater heat flux), and eventually reaching a constant force under steady state gradients. The computer program for calculation of the theoretical values could accommodate the elastic spring modulus of the tie rods, but not the simultaneous action of the thermal-variable prestress force. By equating the initial strain to the thermal strain, a uniform initial seating rod-force could be applied, and the resultant structural response of the restrained test structure to thermal loading could be obtained from the original (Step 1) and the final steady state conditions.

3. The transformers were turned on and each circuit adjusted until a uniform heat flux was produced on the deck. Uniformity was checked by observing the temperature gradients of the receptors when placed at different locations on the bridge deck.

4. When steady state temperatures were achieved (after approximately ten hours of heating), strain gage, thermistor, and dial indicator readings were hand recorded. Recorded values included longitudinal strains and temperatures at previously described points on the stringer and in the slab, strains at the base of the pier to determine any lateral movement at the top of the pier, lateral displacements at the abutments, vertical displacements at the midspans, and ambient temperatures above

and below the deck.

5. After all data were recorded, the heat lamps were turned off; the rods were loosened; the structure was allowed to cool to room temperature; and strain, thermistor, and dial indicator readings were recorded for comparison of cyclic action and instrumentation drift.

DATA REDUCTION

Temperature.—Conversion of thermistor readings to temperature would be generally accomplished by the use of a manufacturer supplied ohm-^{o}C conversion graph or table. In this instance, the internal resistance of the 100-channel stepping unit, needed to interface the large number of thermistors, precluded the reading of thermistor output in ohms. Thus, the output was read in millivolts; equations were developed for ohm-^{o}C conversion at 20^{o} F (11^{o} C) temperature increment ranges; and a computer program written and used for conversion of millivolts to ohms, ohms to ^{o}C, and ^{o}C to ^{o}F.

Strain.—Reduction of observed data obtained from the carbon-steel temperature-compensated SR-4 strain gages required correction for 1) apparent strain, 2) self-temperature-compensation (STC) mismatch, and 3) compensated (nonindicated) thermal strain.

Theoretically a steel-temperature-compensated gage attached to an unrestrained steel specimen should indicate no strain when subjected to a temperature change (20, 21). However, changes in the electrical resistance properties of the gage caused by external temperature change, internal heating, and small differences in material between the gage and specimen, will produce an indicated apparent strain. The electrical resistance-apparent strain relationship is shown on graphs furnished by

the gage manufacturer for data reduction.

STC mismatch is the indicated thermal strain produced by the difference in thermal coefficients of expansion when a self-temperature-compensated gage is mounted on an unrestrained specimen having a thermal coefficient of expansion other than that for which the gage is compensated.

Compensated, or nonindicated, thermal strain is the unit thermal strain which would be induced in an unrestrained specimen subjected to a temperature change, i.e., $\alpha \cdot \Delta T$, the product of the thermal coefficient of expansion and the change in temperature.

Also included in the observed strain is the effect of any restraint to free movement of the specimen. The combination of apparent strain, STC mismatch, and compensated strain coupled with varying degrees of restraint combine to provide solutions to such problems as the experimental determination of the coefficient of thermal expansion (1, 20, 21) as well as strain without stress (very little observed strain), stress without strain (a large magnitude of observed strain), and stress induced by partial restraint.

It should be noted that one may find the term apparent strain used to express any or all of the terms discussed above.

A computer program was developed and used for conversion of observed, as recorded, strain to actual thermally induced strain.

Initial and final dial indicator readings were reduced and combined to provide point deflections and overall structural movement.

RESULTS OF EXPERIMENTAL INVESTIGATION

Temperature Distribution.—Consistent repeated-test results were

obtained; temperature profiles fell within a 6^{o} F (3.3^{o} C) band as shown in the typical experimental profiles of Fig. 5. The difference between the north and south midspan profiles was less than 1^{o} F (0.6^{o} C). These profiles were used as input for computer calculation of theoretical strains. As shown in Fig. 5, the temperature varied from 147^{o} F (64^{o} C) at the top surface of the deck to 125^{o} F (52^{o} C) at the bottom of the deck and 111^{o} F (44^{o} C) at the bottom flange of the stringer.

Ambient temperatures were 114^{o} F (46^{o} C) and 111^{o} F (44^{o} C) at 2 in. (5 cm) and 12 in. (30 cm), respectively, above the deck surface. Below the deck, ambient temperatures were 85^{o} F (29^{o} C) at 12 in. (30 cm) and 84^{o} F (29^{o} C) at 30 in. (76 cm). Ambient temperatures greatly affect temperature profiles. On a still day, the ambient air temperature lies somewhere between the surface temperature of the deck and the temperature at some distance away from the structure. In the laboratory, with the deck surface 60 to 80^{o} F (33 to 44^{o} C) warmer than the air at some distance away from the structure, the ambient air temperature above the deck was approximately the average of the surface temperature and that of the surrounding air, and the ambient temperature beneath the deck was 15 to 20^{o} F (8 to 11^{o} C) above that of the surrounding air.

Strain Distribution.—As previously discussed, the observed strains included apparent strain, STC mismatch, and the effect of tie-rod, abutment and pier restraints. The apparent strain correction is a function of temperature, and is usually assumed to be a linear function within certain temperature ranges. For the tie-rod gages, the correction ranged from zero at 75^{o} F (24^{o} C) to -65 micro strain at 150^{o} F (66^{o} C). The apparent strain correction for all the other gages ranged from zero at 100^{o} F (38^{o} C) to -100 micro strain at 200^{o} F (93^{o} C).

A computer program was developed for reduction of the observed strain to actual thermally induced strain, taking into account the apparent strain, STC mismatch, nonindicated compensated strain, and resistance effect.

Strains for repeated tests fell within a narrow bandwidth similar to that for the temperature profiles. The slight difference between the north and south midspan strains is shown in Fig. 6.

As in the prior study (9, 30) some consistent erratic strains were apparent in the slab. Data obtained from instrument group 3, located 12 in. (30 cm) south of the pier, were not plotted because several gages were unstable or inoperative.

The strain profiles show negative curvature (lengthening of top deck fibers greater than of bottom flange fibers) at the midspan locations, and valid data from instrument group 3 indicate positive curvature at the pier. These relationships are compatible with the temperature profiles (the top of the section warmer than the bottom) and the superposition of abutment-slab thrust.

There was no differential strain at the base of the pier, which indicates that no longitudinal displacement occured at the bearing elevation of the pier, thus resulting in symmetrical longitudinal displacements about the center of the structure. This symmetrical action was substantiated by the dial indicator readings of 0.04 in. (0.102 cm) at each abutment that were virtually identical for each test.

From the data obtained from the cantilever sections of instrument groups 1 and 5, the coefficient of thermal expansion of the concrete was determined to be $4.1 \times 10^{-6}/^{o}$ F ($7.4 \times 10^{-6}/^{o}$ C). The change in value from $3.5 \times 10^{-6}/^{o}$ F ($6.3 \times 10^{-6}/^{o}$ C) as determined in the prior investigation reflects the age effect (approximately 4 years) and other

factors influencing the thermal coefficient of expansion (1, 20).

The experimental temperature profiles were used with the previously described procedure of Emanuel and Hulsey (7) and the computer program developed by Hulsey (16) to obtain the theoretical strains and stresses. The material properties shown in Table 1 were used to calculate the theoretical values of Fig. 7.

The theoretical and (corrected) experimental midspan strains are compared in Fig. 7. As in the prior theoretical (16) and experimental (9, 10, 30) studies, three theoretical cases were analyzed--a) both the slab and the beam in plane stress, b) the slab in plane strain and the beam in plane stress, and c) the slab in some state between plane stress and plane strain (partially restrained) and the beam in plane stress.

For the slab, the closest agreement between experimental and theoretical strains is for case b, the slab in plane strain and the beam in plane stress; whereas for the beam, the closest agreement is for case c, the slab in some state between plane stress and plane strain (partially restrained) and the beam in plane stress.

The observed theoretical vertical deflection at midspans and the horizontal deflections at the abutments were in reasonable agreement--within 15 percent. The observed values were slightly larger than the theoretical values for the vertical deflections and slightly lower for the horizontal deflections. Part of this difference may be explained by the fact that in the theoretical modeling of the bridge, the pier was assumed to resist uplift of the superstructure. Although there was no measurable vertical deflection at the pier, the curved steel rocker and pintle provided no upward restraint. Also, the negative moment

induced at the abutments by the tie-rods increased the negative chamber at the midspans, and may have offset some dead load deflection at the pier. A distorted line diagram of superstructure deformation is shown in Fig. 8.

The theoretical procedure uses the interaction of longitudinal, transverse, and vertical strains and Poisson's ratio in determination of stress; wherein longitudinal strain is the major parameter. Thus, a prediction of stress based on the experimental observations of the investigation is not possible. However, because of the close correlation of the experimental and theoretical midspan strains, theoretical stresses calculated from the observed midspan and pier temperature profiles are believed valid and are presented in Table 2.

Immediately prior to installation of the tie-rods, the test structure was subjected to several cycles of thermal loading--duplicating as closely as possible the maximum power level of the prior study (30)--and the experimental data recorded. This provided a data bank for comparison of the effect of the tie-rods in this study, and the effect of the change in modulus of elasticity and coefficient of thermal expansion from those of the prior study. Again, because of the close correlation of the theoretical and experimental (corrected) strains, comparison of theoretical stresses is believed valid.

With the tie-rods in place, the compressive stress at the top of the deck for cases a, b, and c ranged from 1.7 to 3.5 times the no-tie-rod condition at both the pier and midspans. The compressive stress at the top of the stringer increased by a factor of approximately 1.4, and the tensile stress at the bottom of the stringer decreased by a factor of approximately 2.3.

As compared to the prior study, having a smaller modulus of elasticity and thermal coefficient of expansion, the compressive stress in the concrete at the top of the deck (no-tie-rod condition) increased by a factor of approximately 2.5 and the concrete stress at the bottom of the deck doubled. The compressive stress at the top of the stringer and the tensile stress at the bottom of the stringer each decreased--by a factor of approximately 1.7 and 1.1 to 1.4, respectively.

As discussed in the prior study, integral abutments as contrasted with roller supports, introduce the following effects. As the substructure stiffness increases, changes in the longitudinal stress patterns result primary from the interaction of axial (P/A) and flexural (My/I) stresses produced by the resistance to movement at the abutments. At midspans, the primary influence is an My/I superposition from a moment that induces positive curvature; caused by the resistance of the abutment (piling) to rotation of the superstructure.

In this study, the approach slab (tie-rod) thrust, being below the neutral axis of the composite section, induced an My/I negative curvature superposition. However, because of the proximity of the neutral surface to the deck slab, the compressive P/A stress, being greater than the negative My/I curvature effect on the slab, produced a resultant compressive increase at the top of the deck at the midspans. At the bottom of the stringers, the P/A and My/I stresses, both being compressive stresses, were additive, producing a decrease of tensile stresses at the midspans and pier.

CONCLUSIONS

Based on the correlation of consistent experimental readings and calculated theoretical values, the following conclusions were reached.

1. The theoretical procedure is adequate for a reasonable prediction of abutment-thermal interaction of composite-girder bridge structures subjected to thermal loading.

2. The theoretical longitudinal curvature is somewhat smaller than that observed. This is believed to be a result of the assumption that there is no vertical deflection of the abutments or pier.

3. The observed and theoretical longitudinal strain are in reasonable agreement. Resultant stresses in the test structure, which are functions of longitudinal, transverse, and vertical strains, can be expected to parallel the theoretical values.

4. For the slab, the closest agreement between experimental and theoretical strains is for case b, the slab in plane strain and the beam in plane stress; whereas for the beam, the closest agreement is for case c, the slab in some state between plane stress and plane strain (partially restrained) and the beam in plane stress.

5. The interaction of externally applied abutment forces may increase thermally induced stresses in the slab and stringer by a significant amount--in this instance up to 9 percent of the allowable compressive stress in the concrete and up to 19 percent of the allowable compressive stress in the steel at the midspans.

Further substantiation and modification from field testing of prototype structure to develop rational design criteria for thermal behavior are desirable and feasible.

RECOMMENDATIONS FOR FURTHER STUDY

During the course of any investigation, questions arise as the result of the research. Some of these questions are resolved, but many are beyond the scope of the study and remain unanswered.

The following topics could be of immediate practical value toward development of rational design procedure that would account for thermal behavior of bridge structures and should be explored.

1. Development of a theoretical program capable of taking into account the interaction of bridge weight and upward movement of the piers.

2. Cyclic cooling of the bridge deck to well below freezing temperatures.

3. A study of the effect of diaphragm and beam-slab interaction on lateral torsional buckling and unity of the structure.

4. A study of the effect of shear connector continuity and/or discontinuity on beam-slab interaction.

5. Correlation of experimental laboratory and field prototype temperature profiles.

6. A determination of the thermal coefficient of expansion of reinforced concrete bridge decks, based on the percentage of reinforcing steel.

7. A study of the probabilistic combinations of loading, including environmental loadings, and their relative effect on structural behavior.

Other studies of value to bridge engineers and those in related fields were suggested in the prior studies (9, 10, 16, 30).

APPENDIX I.--REFERENCES

1. Berwanger, C., and Sarkar, A. F., "Effect of Temperature and Age on Thermal Expansion and Modulus of Elasticity of Concrete," Behavior of Concrete Under Temperature Extremes, American Concrete Institute Special Publication SP-39, 1973, pp. 1-22.

2. Berwanger, C., and Symko, Y., "Thermal Stresses in Steel-Concrete Composite Bridges," Canadian Journal of Civil Engineering, Vol. 2, No. 1, 1975, pp. 66-84.

3. Berwanger, C., and Symko, Y., "Finite-Element Solutions for Thermal Stresses in Steel-Concrete Composite Bridges," Experimental Mechanics, Vol. 16, No. 5, May, 1976, pp. 168-175.

4. Black, W., Moss, D. S., and Emerson, M., "Bridge Temperatures Derived from Measurement of Movement," TRRL Report LR 748, Transport and Road Research Laboratory, Crowthorne, Berkshire, England, 1976.

5. Ekberg, C. E., and Emanuel, J. H., "Problems of Bridge Supporting and Expansion Devices and an Experimental Comparison of the Dynamic Behavior of Rigid and Elastomeric Bearings," Final Report, Project 547-S, Engineering Research Institute, Iowa State University, Ames, Iowa, Aug., 1967.

6. Emanuel, J. H., et al., "An Investigation of Design Criteria for Stresses Induced by Semi-Integral End Bents: Phase I--Feasibility Study," Missouri Cooperative Highway Research Program Final Report 72-9, University of Missouri-Rolla, Rolla, Mo., 1973.

7. Emanuel, J. H., and Hulsey, J. L., "Thermal Stresses and Deformations in Nonprismatic Indeterminate Composite Bridges," Transportation Research Record 607, Transportation Research Board, National Academy of Sciences, Washington, D.C., 1976, pp. 4-6.

8. Emanuel, J. H., and Hulsey, J. L., "Temperature Distribution in Composite Bridges," Journal of the Structural Division, ASCE, Vol. 104, No. ST1, Paper 13474, Jan., 1978, pp. 65-78.

9. Emanuel, J. H., and Wisch, D. J., "Thermal Stresses Induced in a Composite Model Bridge Structure," Missouri Cooperative Highway Research Program Final Report 75-2, University of Missouri-Rolla, Rolla, Mo., 1977.

10. Emanuel, J. H., and Wisch, D. J., "Thermal Response of a Continuous Two-Span Composite Bridge Structure," Transportation Research Record 711, Transportation Research Board, National Academy of Sciences, Washington, D.C., 1979, pp. 40-46.

11. Emerson, M., "The Calculation of the Distribution of Temperature in Bridges," TRRL Report LR 561, Transport and Road Research Laboratory, Crowthorne, Berkshire, England, 1973.

12. Emerson, M., "Extreme Values of Bridge Temperatures for Design Purposes," TRRL Report LR 744, Transport and Road Research Laboratory, Crowthorne, Berkshire, England, 1976.

13. Emerson, M., "Temperature Differences in Bridges: Basis of Design Requirements," TRRL Report LR 765, Transport and Road Research Laboratory, Crowthorne, Berkshire, England, 1977.

14. Emerson, M., "Temperature in Bridges During the Hot Summer of 1976," TRRL Report LR 783, Transport and Road Research Laboratory, Crowthorne, Berkshire, England, 1977.

15. Hambly, E. C., "Temperature Distributions and Stresses in Concrete Bridges," Structural Engineering, Vol. 56A, No. 5, May, 1978, pp. 143-148.

16. Hulsey, J. L., "Environmental Effects on Composite-Grider Bridge Structures," thesis presented to the University of Missouri-Rolla, at Rolla, Mo., in 1976, in partial fulfillment of the requirements for the degree of Doctor of Philosophy.

17. Hulsey, J. L., and Emanuel, J. H., "Finite Element Modeling of Climatically Induced Heat Flow," In Numerical Methods for Differential Equations and Simulation (A. W. Bennett and R. Vichnevetsky, eds.), North-Holland, Amsterdam, 1978, pp. 111-114.

18. Hunt, B., and Cooke, N., "Thermal Calculations for Bridge Design," Journal of the Structural Division, ASCE, Vol. 101, No. 9, Sep., 1975, pp. 1763-1781.

19. Lanigan, A. G., "The Temperature Response of Concrete Box Girder Bridges," School of Engineering Report No. 94, thesis presented to the University of Auckland, at Auckland, New Zealand, in 1973, in partial fulfillment of the requirements for the degree of Doctor of Philosophy.

20. Lewis, D. B., "Abutment-Thermal Interaction of a Composite Bridge," thesis presented to the University of Missouri-Rolla at Rolla, Mo., in 1980, in partial fulfillment of the requirements for the degree of Master of Science.

21. Micro-Measurements Division, Measurements Group, "Temperature-Induced Apparent Strain and Gage Factor Variation in Strain Gages," Tech Note TN-128-3, author, Raleigh, N.C., 1976.

22. Priestly, M. J. N., "Design Thermal Gradients for Concrete Bridges," New Zealand Engineering, Vol. 31, No. 9, Sep., 1976, pp. 213-219.

23. Priestly, M. J. N., "Design of Concrete Bridges for Temperature Gradients," Journal of the American Concrete Institute, Vol. 75, No. 5, May, 1978, pp. 209-217.

24. Radolli, M., and Green, R., "Thermal Stresses in Concrete Bridge Superstructures under Summer Conditions," Transportation Research Record 547, Transportation Research Board, National Academy of Sciences, Washington, D.C., 1975, pp. 23-26.

25. Rahman, F., and George, K. P., "Thermal Stress Analysis of Continuous Skew Bridge," Journal of the Structural Division, ASCE, Vol. 105, No. ST7, July, 1979, pp. 1525-1541.

26. Rambhai, P., "Thermal Effects in Concrete Box Girder Bridges," School of Engineering Report No. 139, University of Auckland, Auckland, New Zealand, 1976.

27. Reynolds, J. D., and Emanuel, J. H., "Thermal Stresses and Movements in Bridges," Journal of the Structural Division, ASCE, Vol. 100, No. ST1, Proc. Paper 10275, Jan., 1974, pp. 63-78.

28. Thurston, S. J., "Thermal Stresses in Concrete Structures," Research Report No. 78-21, (Civil Engineering), thesis presented to the University of Canterbury, at Christchurch, New Zealand, in 1978, in partial fulfillment of the requirements for the degree of Doctor of Philosophy.

29. Wah, T., and Kirksey, R., "Thermal Characteristics of Highway Bridges," Highway Research Board Final Report, SwRI Project No. 03-1835, Highway Research Board, National Academy of Sciences, Washington, D.C., 1969.

30. Wisch, D. J., "Thermal Stresses Induced in a Model Composite Bridge Structure," thesis presented to the University of Missouri-Rolla, at Rolla, Mo., in 1977, in partial fulfillment of the requirements for the degree of Master of Science.

31. Zuk, W., "Thermal and Shrinkage Stresses in Composite Beams," Journal of the American Concrete Institute, Vol. 58, No. 3, Sept., 1961, pp. 327-340.

LIST OF CAPTIONS

FIG. 1.—Steel Layout

FIG. 2.—Plan View of Deck Instrumentation Groups

FIG. 3.—Slab Transducer

FIG. 4.—Slab and Stringer Instrumentation

FIG. 5.—Experimental Temperature Profiles

FIG. 6.—Experimental Strain Profiles at Midspans, as Recorded and Temperature Compensated

FIG. 7.—Theoretical and Experimental Strain Profiles at Midspans

FIG. 8.—Distorted Line Diagram of Relative Thermally Induced Superstructure Deflections

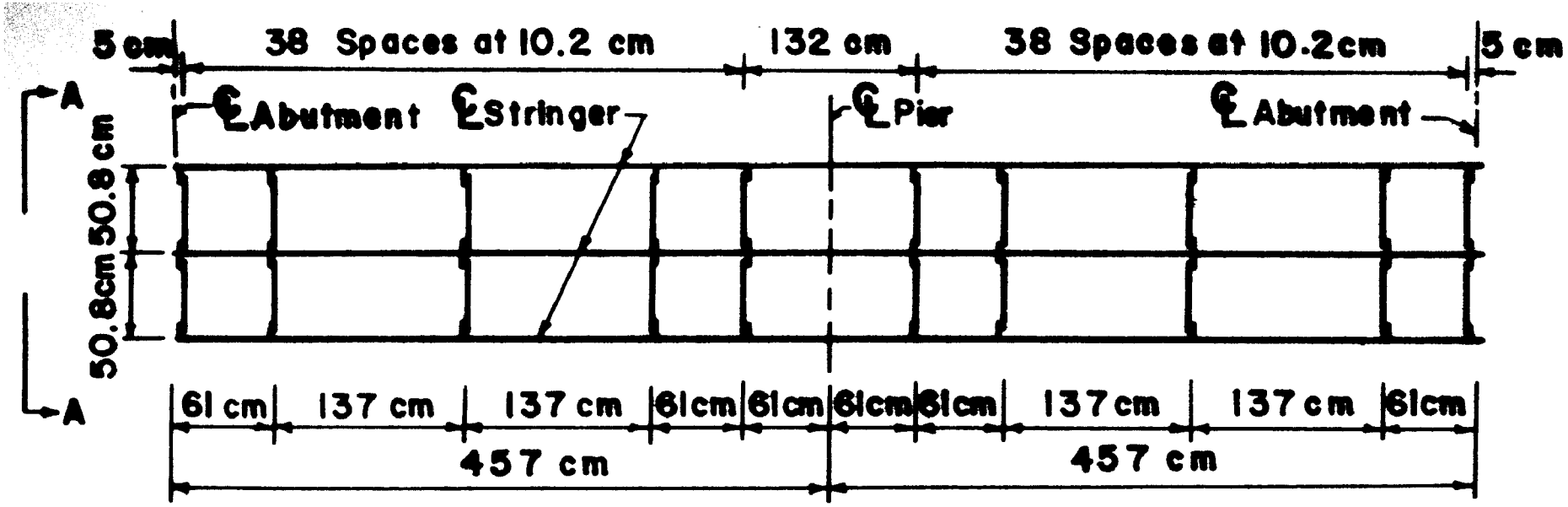

a) Plan View N →

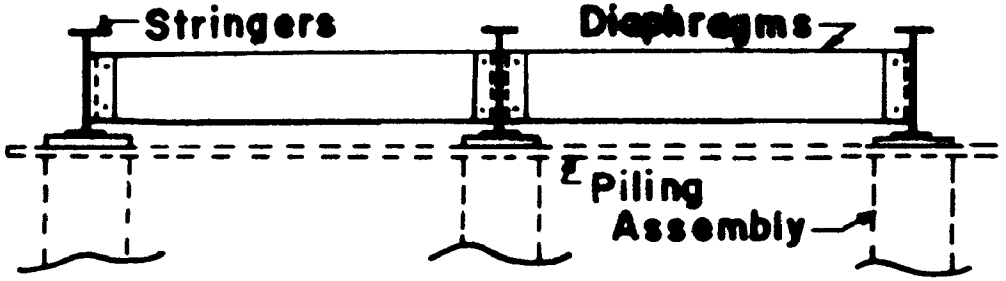

b) Section A-A

Figure 1

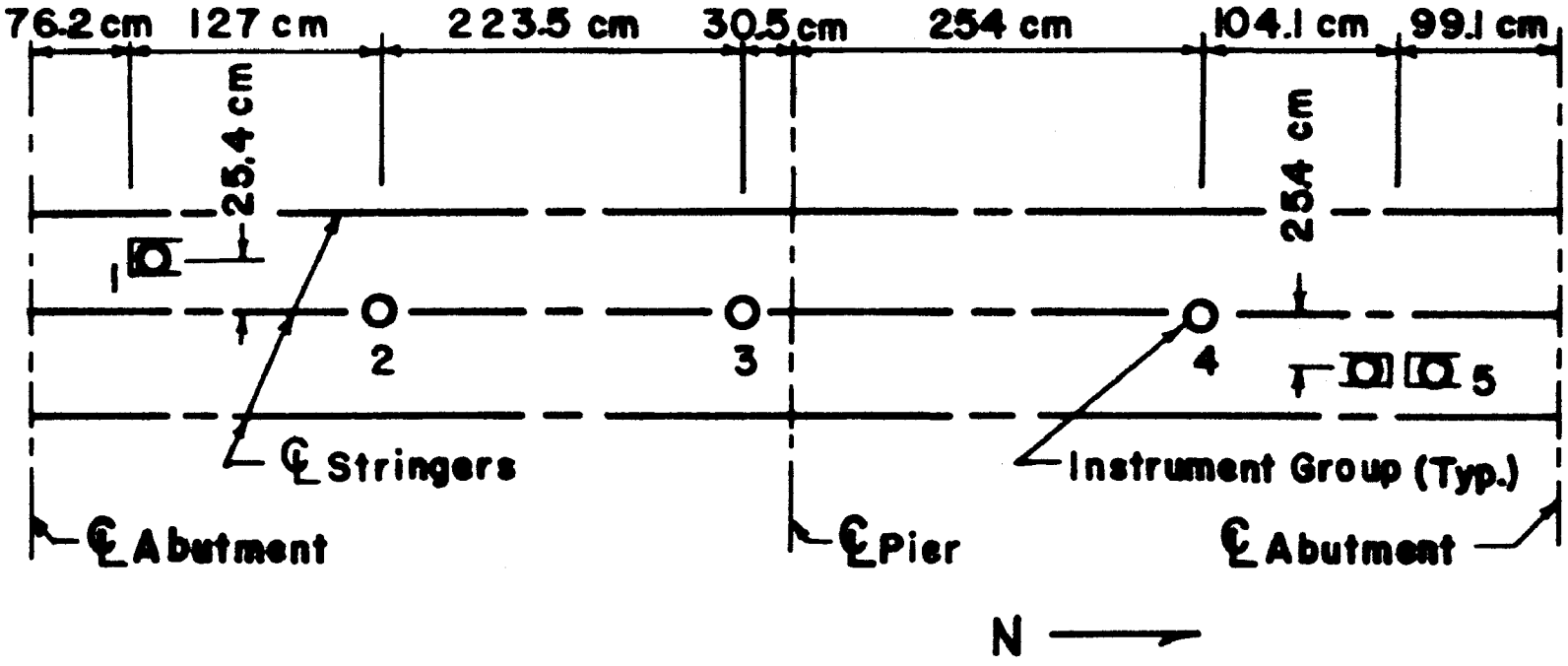
76.2 cm
127 cm
223.5 cm
30.5 cm
254 cm
104.1 cm
99.1 cm
25.4 cm
25.4 cm
1
2
3
4
5
℄ Stringers
Instrument Group (Typ.)
℄ Abutment
℄ Pier
℄ Abutment
N

Figure 2

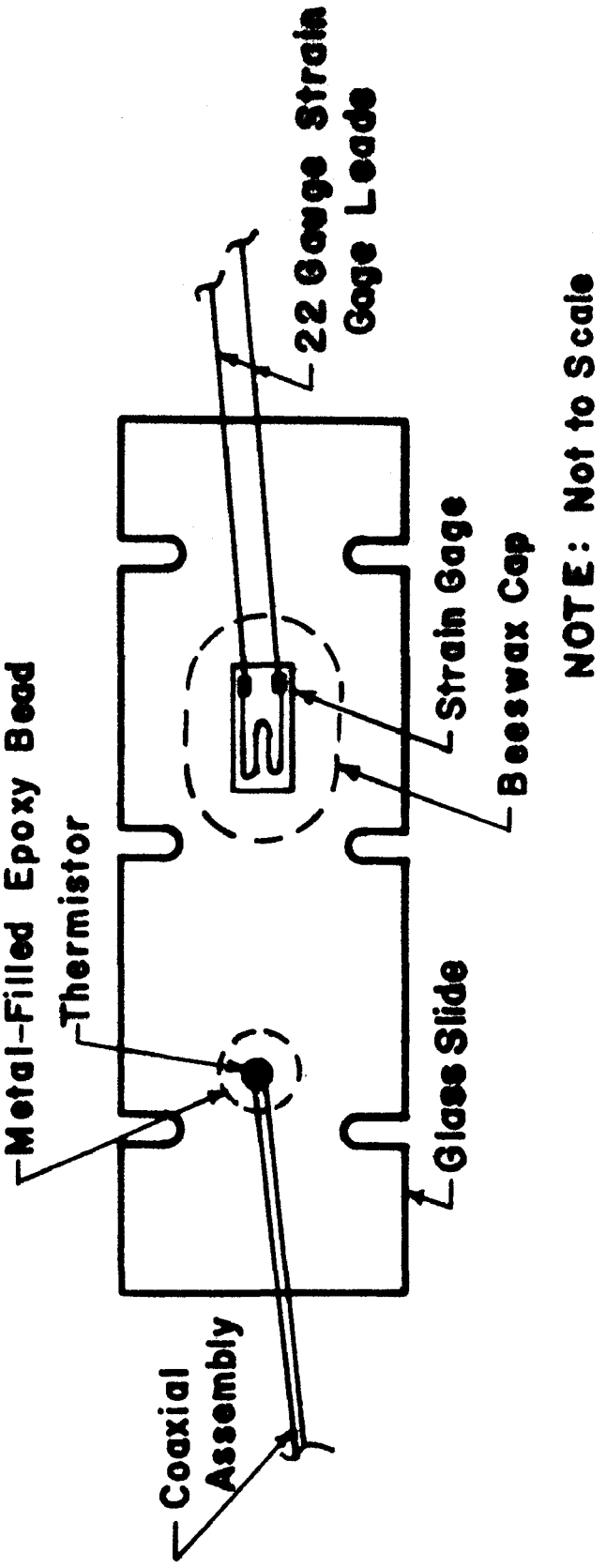
Metal-Filled Epoxy Bead
Thermistor
Coaxial Assembly
Glass Slide
Strain Gage
Beeswax Cap
22 Gauge Strain Gage Leads
NOTE: Not to Scale

Figure 3

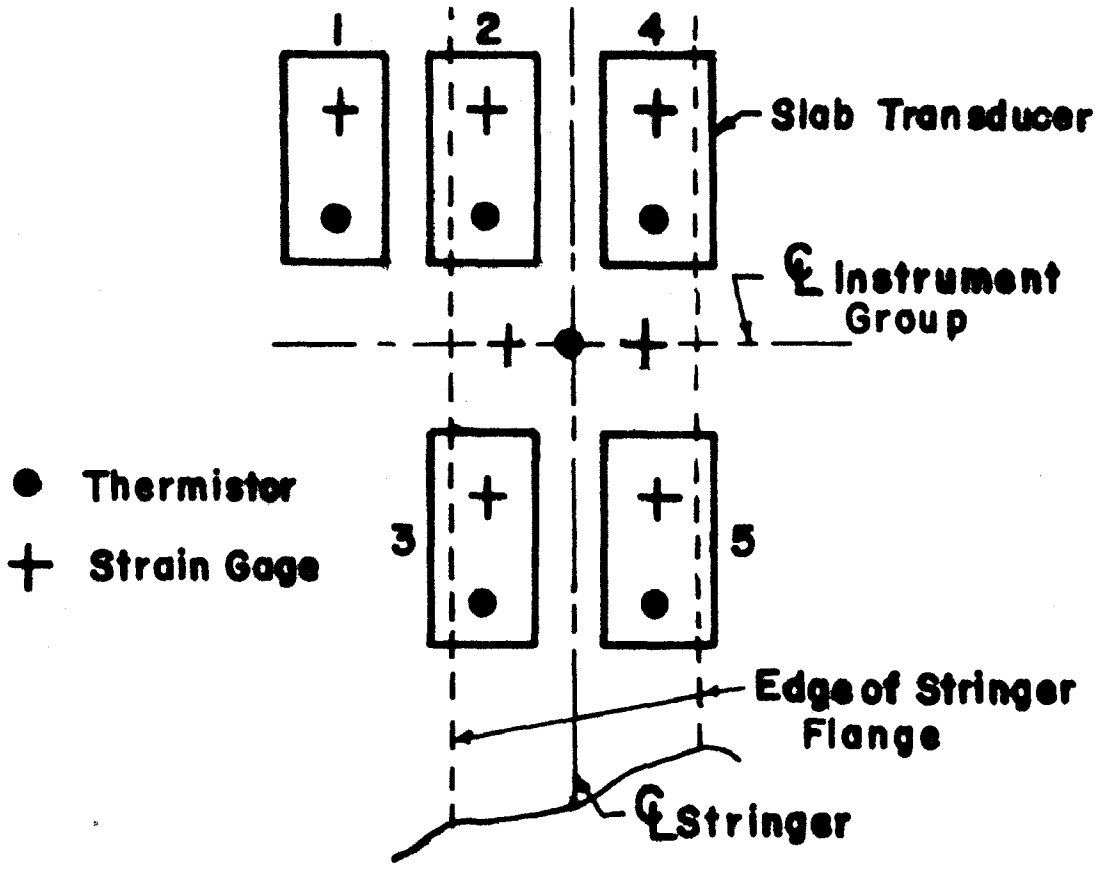

a) Plan View

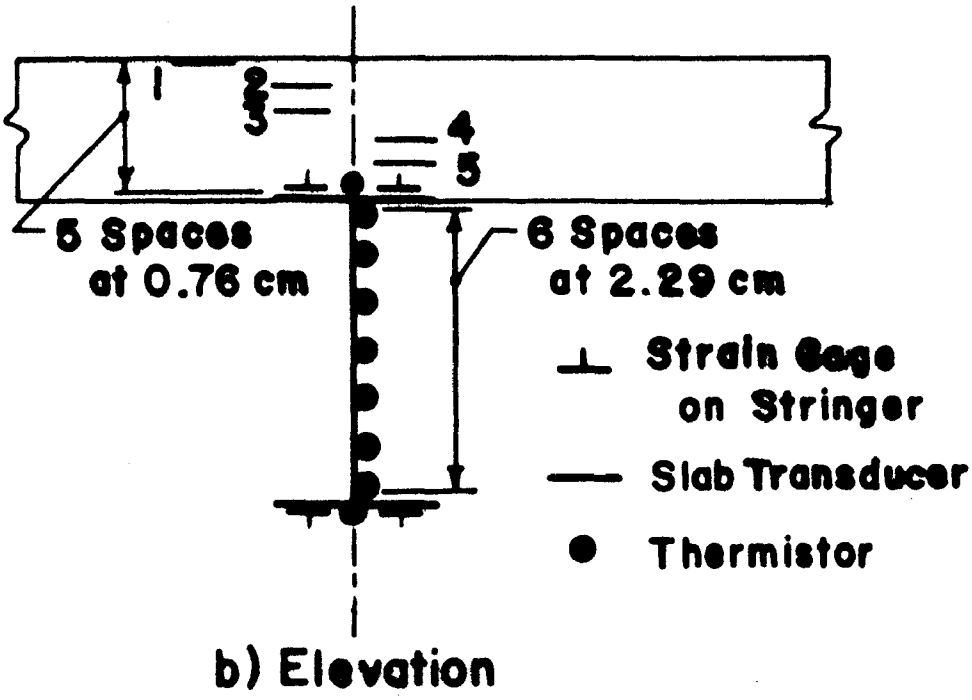

b) Elevation

Figure 4

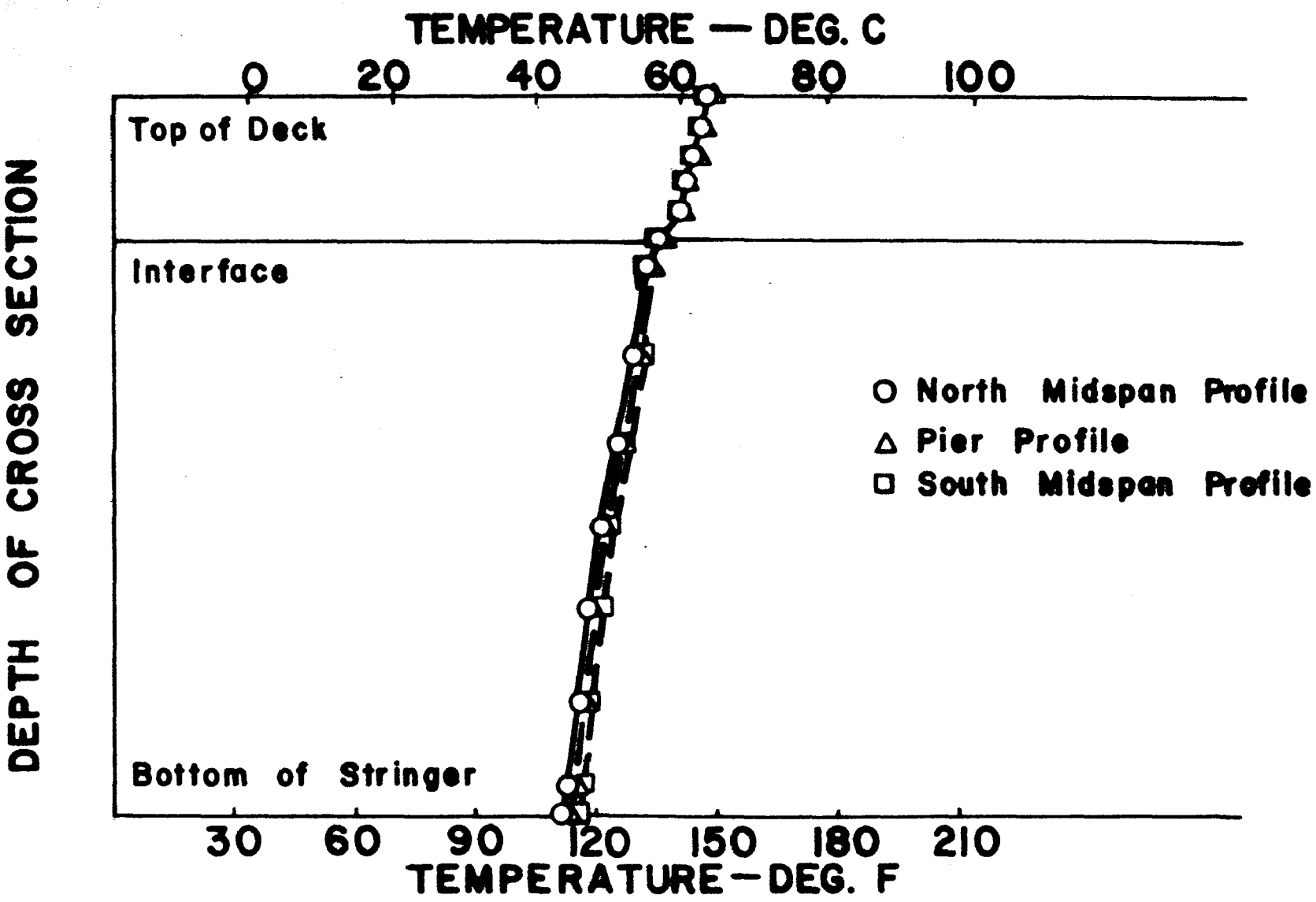
TEMPERATURE — DEG. C
0
20
40
60
80
100
Top of Deck
Interface
Bottom of Stringer
DEPTH OF CROSS SECTION
North Midspan Profile
Pier Profile
South Midspan Profile
30
60
90
120
150
180
210
TEMPERATURE — DEG. F

Figure 5

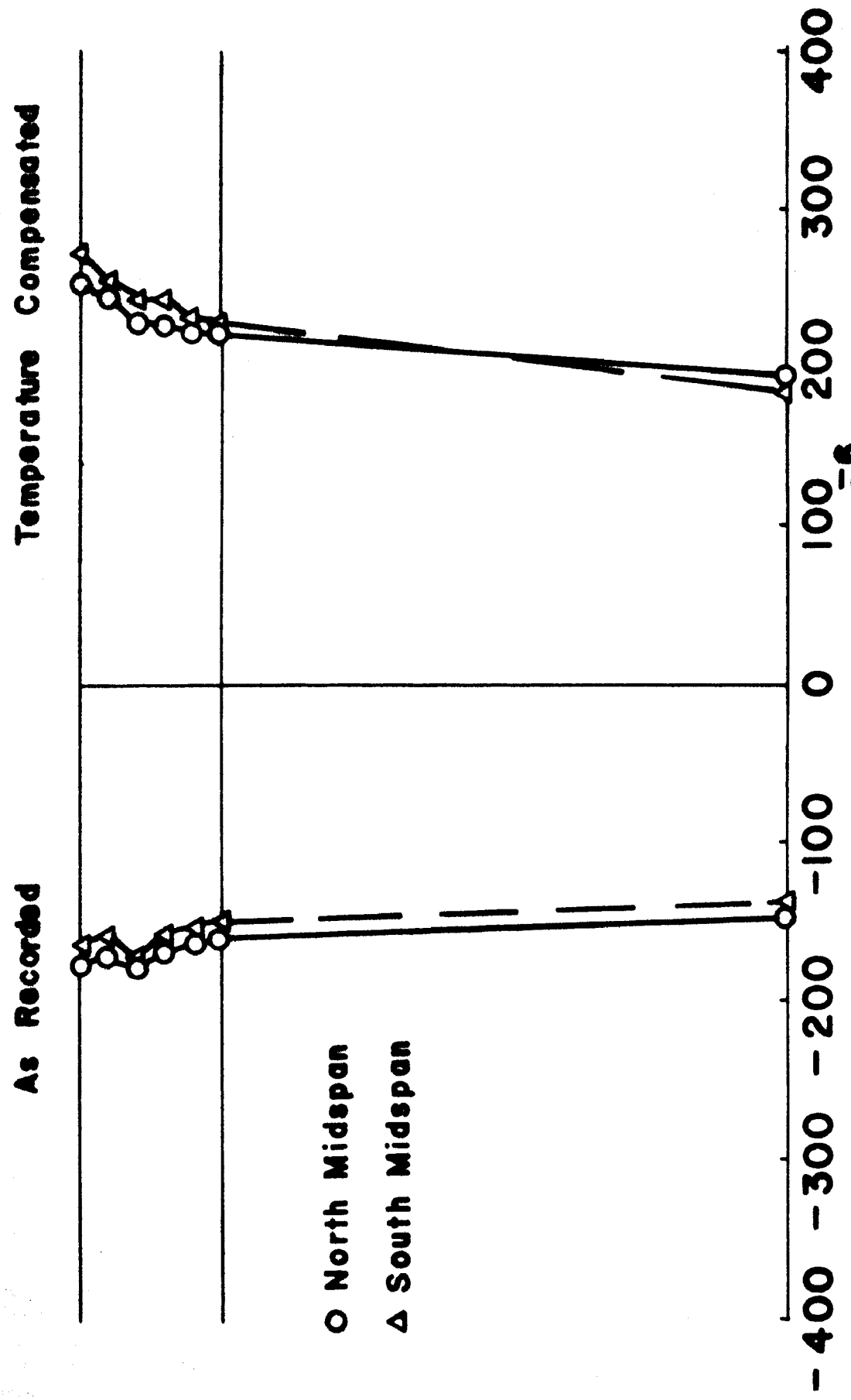
As Recorded
Temperature Compensated
O North Midspan
Δ South Midspan
-400 -300 -200 -100 0 100 200 300 400
UNIT STRAIN x 10⁻⁶

Figure 6

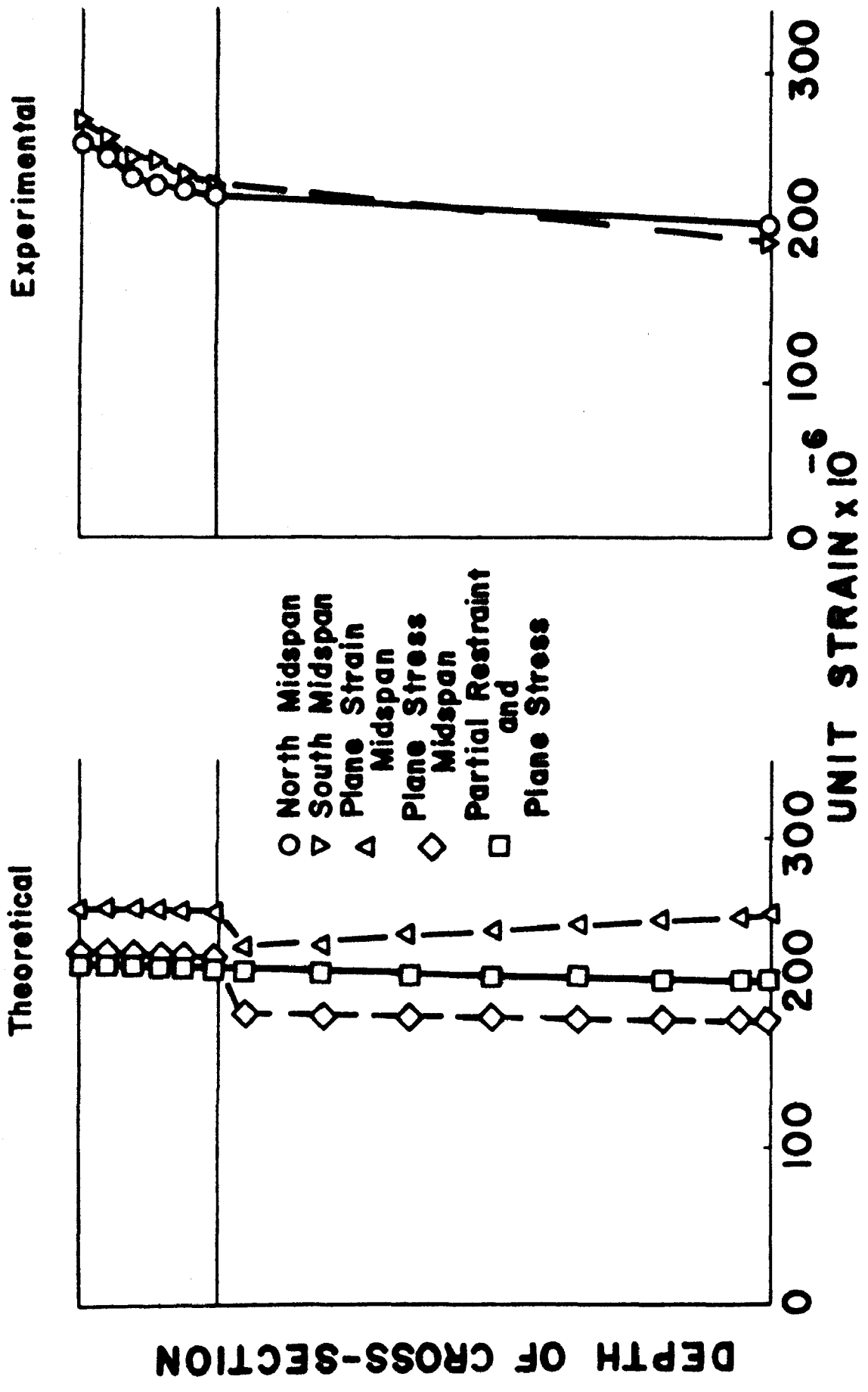
Experimental
Theoretical
North Midspan
South Midspan
Plane Strain Midspan
Plane Stress Midspan
Partial Restraint and Plane Stress
0
100
200
300
UNIT STRAIN x 10^-6
DEPTH OF CROSS-SECTION

Figure 7

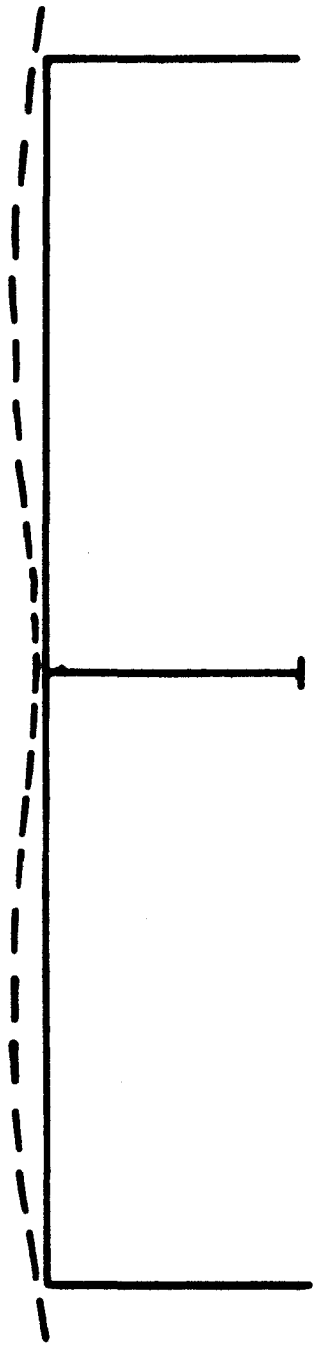

Figure 8

TABLE 1. MATERIAL PROPERTIES

Property (1)	Value	
	Steel (2)	Concrete (3)
Young's Modulus	29.0×10^6 psi	4.5×10^6 psi
	(20.0×10^7 kPa)	(3.1×10^7 kPa)
Poisson's Ratio	0.3	0.18
Coefficient of	$6.5 \times 10^{-6}/^{o}$ F	$4.1 \times 10^{-6}/^{o}$ F
Thermal Expansion	($11.7 \times 10^{-6}/^{o}$ C)	($7.4 \times 10^{-6}/^{o}$ C)

TABLE 2. THEORETICAL STRESSES

Location (1)		case a (2)	case b (3)	case c (4)
Midspans				
Top of slab	(psi)	-177.7	-275.6*	-257.9
	(kPa)	(-1224.4)	(-1898.9)	(-1776.9)
Bottom of slab	(psi)	26.5**	-28.9**	89.5*
	(kPa)	(182.6)	(-199.1)	(616.7)
Top of stringer	(psi)	-3525.0	-2772.0	-4192.0*
	(kPa)	(-24 287.3)	(-19 099.1)	(-28 882.9)
Bottom of stringer	(psi)	-155.9	1821.0*	597.0
	(kPa)	(-1074.2)	(12 546.7)	(4113.3)
Pier				
Top of slab	(psi)	-195.1	-297.0*	-281.1
	(kPa)	(-1344.2)	(-2046.3)	(-1936.8)
Bottom of slab	(psi)	25.9**	-29.7**	88.7*
	(kPa)	(178.5)	(-204.6)	(611.1)
Top of stringer	(psi)	-3529.0	-2777.0	-4198.0*
	(kPa)	(-24 314.8)	(-19 133.5)	(-28 924.2)
Bottom of stringer	(psi)	270.6	2374.0*	1167.0
	(kPa)	(1864.4)	(16 356.9)	(8040.0)

*Maximum of the three cases.

**Magnitude too small to be significant.

VITA

David Bradley Lewis was born the 4th day of May, 1956, in Bonne Terre, Missouri. He received his primary education in Albuquerque, New Mexico, and his secondary education in Farmington, Missouri. In August, 1974, he enrolled at Mineral Area College at Flat River, Missouri, and received an Associate of Arts Degree in May, 1976. By December, 1978, he had received a Bachelor of Science Degree in Civil Engineering at the University of Missouri-Rolla and started his pursuit of a Master of Science Degree.

He held a Graduate Teaching Assistantship in the Civil Engineering Department of the University of Missouri-Rolla for the period of January, 1979, to May, 1980. He was active in ASCE being president and vice-president of the student chapter. He is an Engineer-in-Training in the State of Missouri, and a member of Chi Epsilon and Tau Beta Pi, engineering honor societies.

APPENDIX A

EXPERIMENTAL DETERMINATION OF THE THERMAL COEFFICIENT OF EXPANSION

APPENDIX A

EXPERIMENTAL DETERMINATION OF THE THERMAL COEFFICIENT OF EXPANSION

Experimental evaluation of thermally induced stresses first requires an accurate determination of the effective coefficient of thermal expansion of the component materials of the structure. Thus, to verify the applicability of procedures reported in the literature, the following preliminary study of homogeneous materials with accepted thermal coefficients was conducted.

Two rods 1/2-in. (12.7-mm) in diameter by 24-in. (61-cm) long were selected for study; one of aluminum and one of structural aluminum (2024-T4). Both were readily available, and their accepted coefficients of thermal expansion are readily obtained in the literature. A 1/2-in. (12.7-mm) in diameter by 24-in. (61-cm) long steel rod (1018) was selected for correlation of the observed data.

The rods were mounted as cantilever beams in a 1 x 2 x 2-ft (30 x 60 x 60-cm) sealed plywood heat chamber. Transducer units consisting of one Micro-Measurements FAE-25-12-56EWL SR-4 steel-temperature-compensated strain gage and one Fenwal Electronics UUA 33J1 thermistor were mounted on each rod 4 in. (10 cm) from the free end. Because of the conductivity of the rod and the proximity of the gage and thermistor, the thermistor measured the temperature of both the rod and the strain gage. Two General Electric Model 250R40 110-volt infrared heat lamps, mounted within the heat chamber and connected in series to a 240-volt variable transformer, were used to provide the thermal loading.

The thermistors were connected to a digital voltmeter (Dana Model 5400) through a 20 channel Baldwin-Lima-Hamilton Model 225 switching unit. The resistance of each of the thermistors was indicated by the volt-ohm meter. The temperature was determined for each thermistor by the use of the temperature-resistance graph furnished by the manufacturer. Strains were measured by the means of a Baldwin-Lima-Hamilton Model 120C strain indicator. A Baldwin-Lima-Hamilton Model 225 10 channel switch and balance unit was used to interface the strain gages and strain indicators.

At the start of each test the temperature and the initial strains were recorded for each of the three rods, and the heat lamps were turned on. After steady state temperatures were obtained, generally about 150° F (66° C) in approximately three hours, temperatures and strains were again recorded. The lamps were turned off, the heat chamber opened and the rods allowed to return to room temperature, after which the temperatures and strains were again recorded for comparison with initial values. A series of ten tests was conducted to check reproducibility.

No change in strain should be observed in a self-temperature-compensating strain gage subjected to a temperature change when freely suspended or when mounted to an unrestrained specimen of the material for which the gage was compensated and subjected to a uniform thermal gradient. However, a change in strain will occur. Thus, it is obvious that other factors are involved. The primary factors are apparent strain and self-temperature-compensating (STC) mismatch.

The resistivity of an electric resistance strain gage, either unrestrained or strained, is also a function of gage temperature. Thus, a change in gage temperature, either externally or internally

induced, will generally cause a resistance change in the gage and an indicated change in strain, which is referred to as apparent strain to distinguish it from strain caused by an applied stress. The magnitude of this apparent strain may be caucluated by using the correction equation for each particular gage lot, in this instance:

$$\varepsilon_{app(st)} = -73.53 + 2.64(T) - 2.8 \times 10^{-2}(T^2) + 8.21 \times 10^{-5}(T^3) - 6.65 \times 10^{-8}(T^4) \quad (1)$$

wherein $\varepsilon_{app(st)}$ is the apparent strain correction for the type of steel (1018) for which the gage was compensated in micro in./in. and T is the temperature of the gage in ^{o} F at the time of strain reading.

STC mismatch results when a strain gage is mounted on a material other than that used in obtaining the data for development of the apparent strain correction equation. In this investigation STC mismatch would occur for both aluminum rods, but not for the steel rod, as the apparent strain correction was developed for the strain gage mounted on this type of steel. The equation for correction of STC mismatch for the aluminum rods is:

$$\varepsilon_{app(al)} = \varepsilon_{app(st)} + (\alpha_{(al)} - 6.7)(\Delta T) \quad (2)$$

where $\varepsilon_{app(al)}$ is the apparent strain correction for the specified aluminum rod in micro in./in.; $\varepsilon_{app(st)}$ is the apparent strain correction for the type of steel (1018) for which the gage was compensated in micro in./in.; $\alpha_{(al)}$ is the thermal coefficient of expansion of the specified aluminum rod in micro in./in.^{o} F; the numerical value, 6.7, is the thermal coefficient of the 1018 steel for which the gage was compensated; and ΔT is the change in temperature in ^{o} F.

Rearranging terms:

$$\alpha_{(al)} = \frac{-\varepsilon_{app(st)} + \varepsilon_{app(al)}}{\Delta T} + 6.7 \qquad (3)$$

in which the terms are defined for Eq. 2.

The step-wise development of the results of the five tests summarized in Table I is illustrated for test number 4 in the following.

1) Strain gages balanced (to zero) and initial temperature of 73^{o} F (23^{o} C) recorded.

2) Steady state temperature (after heating to approximately 142^{o} F 61^{o} C) and strains recorded.

3) The change in temperature, ΔT, and the change in strain, calculated (final - initial).

4) The apparent strains are calculated. The apparent strain correction for the aluminum is the change in strain, $\Delta\varepsilon$, from step 3. The apparent strain correction for the 1018 steel used in this study may be obtained from Eq. 1 or taken as $\Delta\varepsilon$ of the steel, as the two values should be equal because the steel rod of this study was the same type (1018) as that for which the gage was compensated.

5) Knowing the apparent strain correction for the steel (1018) and its coefficient of thermal expansion, 6.7, the apparent strain correction for the specified aluminum rod, and the change in temperature, ΔT, the coefficient of thermal expansion for each of the aluminum rods is calculated by Eq. 3 as being 12.9×10^{-6} in./in.^{o} F ($23.2 \times 10^{-6}/^{o}$ C) and 13.2×10^{-6} in./in.^{o} F ($23.8 \times 10^{-6}/^{o}$ C), respectively.

The accepted coefficients for this study were: for steel--6.7×10^{-6} in./in.^{o} F ($12.1 \times 10^{-6}/^{o}$ C); for structural aluminum--12.9×10^{-6}

in./in.^{o} F (23.2 x $10^{-6}/^{o}$ C); and for aluminum--13.2 x 10^{-6} in./in.^{o} F (23.8 x $10^{-6}/^{o}$ C). These are comparable to the experimental values shown in Table I.

TABLE I

EXPERIMENTAL DATA

	Steel				Structural Aluminum				Aluminum			
Test	Strain Read	$\varepsilon_{app(st)}$	ΔT	$\alpha_{(st)}$	Strain Read	$\varepsilon_{app(al)}$	ΔT	$\alpha_{(al)}$	Strain Read	$\varepsilon_{app(al)}$	ΔT	$\alpha_{(al)}$
(1)	(2)	(3)	(4)	(5)	(6)	(7)	(8)	(9)	(10)	(11)	(12)	(13)
1	-45	-54.0	65.3	6.9	347	365.0	68.0	12.6	392	406.0	71.9	13.0
2	-39	-61.9	69.4	7.0	336	333.6	62.6	12.9	392	388.9	69.4	13.2
3	-37	-63.0	76.0	7.0	374	376.2	69.7	12.9	428	430.5	75.9	13.2
4	-45	-56.3	69.9	6.9	350	349.1	64.3	12.9	395	395.0	69.3	13.2
5	-45	-57.4	70.7	6.9	383	393.8	73.2	12.8	412	424.5	74.8	13.0

APPENDIX B

DETERMINATION OF THE STATIC MODULUS OF ELASTICITY OF CONCRETE IN COMPRESSION

APPENDIX B

DETERMINATION OF THE STATIC MODULUS OF ELASTICITY OF CONCRETE IN COMPRESSION

The calculation of theoretical values for correlation with experimental results required an accurate value of the modulus of elasticity of the concrete. Although the modulus of elasticity was determined from compressive cylinder test at the time of construction a few years ago, it is well known that the mechanical properties of concrete vary as a result of many factors, one of which is age.

Thus, it was deemed necessary to experimentally determine the modulus of elasticity, E, of the concrete of the test structure at the time of this investigation.

Four standard 6 x 12-in. (15 x 30-cm) cylinders cast at the time of construction had been stored on the superstructure deck. The cylinders were capped in accordance with ASTM Standard C617. Two cylinders were used for determination of the ultimate compressive strength, f'_c, in accordance with ASTM Standard C39, and two were used for determination of the modulus of elasticity in accordance with ASTM Standard C460-65.

One cylinder reached an ultimate load of 198,000 lb (882,000 N), or 7,000 psi (47,600 kPa), and the other exceeded the 200,000 lb (890,000 N) capacity of the testing machine.

Four cycles of loading and unloading from 0 to 100,000 lb (0 to 445,450 N) were applied to each of the remaining two cylinders at 10,000 lb (44,550 N) load increments.

The load-deflection data were averaged and reduced to values of stress and strain for the plotting of a stress-strain curve by means

of a least squares fit. The secant modulus of elasticity at $\frac{1}{2}f'_c$ was determined to be 4.45×10^6 psi (3.03×10^7 kPa). The value determined by the equation of ASTM Standard C460-65 ($E = (S_2 - S_1)/(\varepsilon_2 - 0.000050)$, wherein E is the chord modulus of elasticity; S_2 is the unit stress corresponding to 40 percent of ultimate load; S_1 is the unit stress corresponding to a longitudinal strain of 50 micro in./in.; and ε_2 is the longitudinal strain produced by stress S_2) was 4.35×10^6 psi (2.96×10^7 kPa). The value of the modulus of elasticity reported in the prior investigation four years ago was 3.0×10^6 psi (2.04×10^7 kPa).

APPENDIX C

THEORETICAL STRESSES

APPENDIX C

THEORETICAL STRESSES

The objective of this study was to correlate experimental and theoretical stresses induced in a composite bridge structure as a result of abutment-thermal interaction. As previously explained, prior to installation of the tie-rods the test structure was subjected to several cycles of thermal loading--repeating as closely as possible the maximum power level loading of the prior study--and the experimental data recorded. This provided a data bank for comparison of a) the no-tie-rod and the tie-rod conditions of this investigation, and b) the no-tie-rod condition of this investigation and that of the prior study, which had smaller values for both the modulus of elasticity and the coefficient of thermal expansion.

The experimental no-tie-rod condition and the theoretical strains were in close agreement and, as previously discussed, comparison of the theoretical stresses is believed valid. The effect of the tie-rod for cases a and b above are discussed in the results of the experimental investigation. However, the page limitation restrictions prevented inclusion of the numerical values of theoretical stresses.

Thus, they are tabulated in Tables II and III, to permit comparison should the reader desire.

TABLE II

THEORETICAL STRESSES FOR PROPERTIES AT THE TIME OF THIS INVESTIGATION (NO TIE-ROD-CONDITION)

Location (1)		case a (2)	case b (3)	case c (4)
Midspans				
Top of slab	(psi)	-50.3	-84.5	-90.6*
	(kPa)	(-346.6)	(-582.2)	(-624.2)
Bottom of slab	(psi)	151.0	122.9	239.0*
	(kPa)	(1033.5)	(846.8)	(1646.7)
Top of stringer	(psi)	-2594.0	-1774.0	-3056.0*
	(kPa)	(-17 872.7)	(-12 222.9)	(-21 055.8)
Bottom of stringer	(psi)	796.0	186.3	1363.0*
	(kPa)	(5484.4)	(1283.6)	(9391.1)
Pier				
Top of slab	(psi)	-55.3	-172.3*	-126.3
	(kPa)	(-381.0)	(-1187.1)	(-870.2)
Bottom of slab	(psi)	150.8	119.7	237.7*
	(kPa)	(1039.0)	(824.7)	(1637.8)
Top of stringer	(psi)	-2595.0	-1795.0	-3046.0*
	(kPa)	(-17 879.6)	(-12 367.6)	(-20 986.9)
Bottom of stringer	(psi)	916.9	4024.0*	2238.0
	(kPa)	(6317.4)	(27 725.4)	(15 419.8)

*Maximum of the three cases.

TABLE III

THEORETICAL STRESSES FOR PROPERTIES
OF THE PRIOR STUDY

Location (1)		case a (2)	case b (3)	case c (4)
Midspans				
Top of slab	(psi)	9.0	-31.0	-47.0*
	(kPa)	(62.0)	(-214.0)	(-324.0)
Bottom of slab	(psi)	140.0*	119.0	264.0
	(kPa)	(966.0)	(821.0)	(1822.0)
Top of stringer	(psi)	-4380.0	-3290.0	-4890.0*
	(kPa)	(-30 222.0)	(-22 700.0)	(-33 740.0)
Bottom of stringer	(psi)	1190.0	1910.0*	1250.0
	(kPa)	(8211.0)	(13 179.0)	(8625.0)
Pier				
Top of slab	(psi)	11.0	-42.0	-44.0*
	(kPa)	(76.0)	(-290.0)	(-304.0)
Bottom of slab	(psi)	140.0	114.0	264.0*
	(kPa)	(966.0)	(787.0)	(1822.0)
Top of stringer	(psi)	-4380.0	-3340.0	-4880.0*
	(kPa)	(-30 222.0)	(-23 046.0)	(-33 672.0)
Bottom of stringer	(psi)	1150.0	2940.0*	1150.0
	(kPa)	(7935.0)	(20 286.0)	(7435.0)

*Maximum of the three cases.